Contents lists available at SciOpen

Food Science and Human Wellness

journal homepage: https://www.sciopen.com/journal/2097-0765

China Food Publishing Co.

Unraveling the mechanism of *Ligilactobacillus salivarius* AR612 in response to glucose stress from the insights of genome and transcriptome analysis

Yong Yang, Xin Song, Guangqiang Wang, Yongjun Xia, Zhiqiang Xiong, Lianzhong Ai*

Shanghai Engineering Research Center of Food Microbiology, University of Shanghai for Science and Technology, Shanghai 200093, China.

ARTICLE INFO

Article history:
Received 30 January 2024
Received in revised form 2 April 2024
Accepted 19 June 2024

Keywords:
Ligilactobacillus salivarius AR612
Whole genome
Transcriptome
Glucose stress
Differentially expressed genes

ABSTRACT

This study examined the potential response mechanisms of *Ligilactobacillus salivarius* AR612 to glucose stress through whole-genome and comparative transcriptome analysis. We obtained the basic genome information of *L. salivarius* AR612. The full genome length of *L. salivarius* AR612 was 1 970 245 bp, with a GC content of 33.01% and 1 894 coding genes. Moreover, we identified many genes associated with genetic adaptations to various stress factors, including temperature, pH, osmotic pressure, bile salts, and oxidative stress. Physiological analysis revealed that the growth and morphology of AR612 changed significantly under glucose stress, with a decrease in the maximum growth and irregular cell morphology. Furthermore, a comparison of transcriptome data indicated that glucose stress induced changes in the number of differential genes. Moreover, AR612 could respond to extracellular glucose stress by changing the expression of genes related to cell morphology, carbohydrate metabolism, amino acid metabolism, fatty acid synthesis, and nucleotide metabolism. This study provides valuable theoretical insights for future research on the adaptation of *L. salivarius* AR612 to nutritional stress and its application in industrial processes.

1. Introduction

Probiotics are defined as live microorganisms that, when administered in adequate amounts, may exert a beneficial effect on the health of the host[1]. As important intestinal microorganisms, probiotics play a vital role in maintaining body homeostasis by inhibiting pathogenic bacterial growth, reducing cholesterol levels, regulating immunity, improving gastrointestinal flora, promoting nutrient absorption, and exerting antioxidant effects[2]. For these functional properties to be effective, probiotics must enter the gastrointestinal tract in a viable state. However, probiotics encounter environmental conditions that can be detrimental to their survival, including temperature fluctuations, acid-base imbalances, osmotic pressure variations, oxidation, and repeated freeze-thaw cycles[3-4]. These factors may lead to a series of physiological changes in the genotype and phenotype of lactic acid bacteria (LAB).

Ongoing research on the relationship between probiotics and gut microbiome health has revealed that the nutritional needs and preferred growth environments of probiotics vary from strain to strain[5]. Nutritional stress resulting from nutrient scarcity in the probiotic niche is frequently identified as a specific limiting factor. Systems biology and multi-omics technologies can be effectively used to study mechanisms underlying the responses of probiotics to nutritional stress. Dressaire et al.[6] employed transcriptomics and proteomics to investigate the response mechanism of *Lactococcus lactis* to isoleucine deficiency.

Glucose is the most common source of carbon and energy for probiotics. In the absence of glucose, probiotics experience starvation stress and are required to catabolise amino acids or other sugars as alternative sources of carbon and energy[7]. Conversely, high glucose concentrations create a hypertonic environment, leading to oxidative

* Corresponding author at: Shanghai Engineering Research Center of Food Microbiology, University of Shanghai for Science and Technology, Shanghai 200093, China.
E-mail address: ailianzhong1@126.com (L.Z. Ai)
Peer review under responsibility of Beijing Academy of Food Sciences.

SciOpen Publishing services by Tsinghua University Press

http://doi.org/10.26599/FSHW.2024.9250350

stress and inducing the production of large amounts of reactive oxygen species (ROS), which result in cellular damage. Using transcriptomics, Wang et al.[8] investigated the effects of 3 glucose concentrations (2%, 40%, and 70%, *m*/*V*) on the cell morphology, ergosterol and linoleic acid synthesis of *Zygosaccharomyces rouxii*. Previous studies integrated genomics, proteomics, and metabolomics to analyse the adaptation mechanism of *Lactobacillus casei* under glucose-restricted conditions and identified a series of key differential proteins and metabolites involved in the response to glucose restriction. The authors have provided an omics basis for improving the tolerance of *L. casei* to nutritional stress[9-10]. Thus, examining the responses of probiotics to nutritional stress is crucial for designing and optimising their growth and fermentation conditions, serving as a valuable guide for subsequent high-density culturing.

Ligilactobacillus salivarius is a type of LAB recognised by the European Food Safety Authority (EFSA) as having a qualified presumption of safety and is widely applied in various fields[11-12]. AR612, a strain of the probiotic *L. salivarius*, was isolated in our laboratory. Using whole-genome sequencing, we examined the response mechanism of AR612 under glucose stress through transcriptome sequencing. The findings of this study provide a valuable reference for future functional studies.

2. Materials and methods

2.1 *L. salivarius AR612 culture condition*

L. salivarius AR612 (stored at the China General Microorganism Storage Center, CGMCC No. 28709) was incubated in fresh deMan, Rogosa, Sharpe (MRS) broth (Beijing Solarbio Science & Technology Co., Ltd., Beijing, China) using a volume fraction of 1% under static culture at 37 °C until reaching the mid-logarithmic stage. Subsequently, AR612 cells were harvested through centrifugation at 8 000 × *g* and stored at –80 °C for genomic DNA extraction. The glucose stress experiment was performed as follows. AR612 was cultured in MRS medium for 12 h. Bacterial solution was then inoculated into MRS medium containing 1.5 g/L (low glucose group, L), 20 g/L (control group, M), and 150 g/L (high glucose group, H) glucose, respectively. After static culture at 37 °C for 3.5 h (T1) and 12 h (T2), the bacterial liquid was centrifuged at 12 000 × *g* for 5 min at 4 °C to extract RNA. RNA extraction was performed in accordance with the TIANGEN RNA extraction kit protocol (TIANGEN Biotech Co., Ltd., Beijing, China).

2.2 *Determination of pH and growth curve of AR612*

The pH value of the *L. salivarius* AR612 supernatant was measured using a pH meter (Mettler-Toledo, Grelfensee, Switzerland). The biomass concentration of *L. salivarius* AR612 was measured using an ultraviolet visible spectrophotometer (UV2600, UNICO, USA).

2.3 *Preparation of scanning electron microscopy (SEM) sample*

The SEM sample was prepared following the method reported by Parlindungan et al.[13] with some modifications. The obtained glucose-stressed cells of *L. salivarius* AR612 were mixed with glutaraldehyde (2.5%, pH 6.8) and fixed for 12 h at 4 °C. After fixation, the samples were rinsed in 0.2 mol/L phosphoric acid buffer (pH 7.0) 3 times for 15 min each time. Then, the samples were dehydrated with gradient concentrations of ethanol solution (30%, 50%, 70%, 80%, 90%, and 95%, *V*/*V*). Each concentration was applied for 15 min, followed by 2 20-min treatments with 100% ethanol. The samples were then treated with a mixture of ethanol and isoamyl acetate (1:1, *V*/*V*) for 30 min, followed by isoamyl acetate overnight. The treated samples were observed under a scanning electron microscope (HITACHI SU8010) after critical point drying and coating. The length (*l*) and diameter (*d*) were measured for 15 to 30 AR612 cells. The average cell volume (*V*) was calculated using the method reported by Parlindungan et al.[14]. In brief, the functional equation of the average cell volume and radius ($r = d/2$) and height ($h = l - 2r$) is as follows: $V = 4/3\pi r^3 + \pi r^2 h$.

2.4 *Genomic DNA and total RNA extraction*

Genomic DNA was extracted from *L. salivarius* AR612 using the Wizard® genomic DNA purification kit (Promega, USA) in accordance with the manufacturer's protocol. The integrity and size of the DNA samples were assessed using 0.6% agarose electrophoresis. A Nanodrop 2000 (Thermo Fisher Scientific, MA, USA) was used to quantify DNA, and a high-quality DNA sample was used for subsequent library sequencing. The TRIzol method was used to extract total RNA from different glucose stress groups. After the removal of genomic DNA, the quality of total RNA was determined using 1% agarose electrophoresis and an Agilent 5300 biological analyser. RNA quantification was performed using a Nanodrop 2000, and high-quality RNA samples were used for subsequent library construction.

2.5 *Library construction, sequencing, and quality control*

The genome of *L. salivarius* AR612 was sequenced using the PacBio RS II platform and Illumina HiSeq platform at Majorbio Bio-Pharm Technology Co., Ltd. (Shanghai, China). Four SMRT cells Zero-Mode Waveguides (ZMW) sequencing arrays were used in the PacBio platform to generate the subreads set. For RNA sequencing, the cDNA library was constructed using the TruSeq™ Stranded Total RNA Library Prep Kit for Illumina following the manufacturer's instructions. The library was then paired-end sequenced using the Illumina NovaSeq 6000 platform (Illumina, San Diego, CA., USA). The quality of the sequencing data was assessed using FastQC (v0.11.2). To ensure the quality and reliability of transcriptome data, the original sequencing data should be filtered. This process involved removing adapter sequences from reads, deleting non-A, G, C, and T bases at the 5′ end, and excluding low-quality reads.

2.6 *Genome and transcriptome annotation*

High-quality sequences obtained through genome sequencing were assembled and spliced using Unicycler (v0.4.8) software. First, the BLAST (https://blast.ncbi.nlm.nih.gov/Blast.cgi) and PLSDB databases (https://ccb-microbe.cs.uni-saarland.de/plsdb/) were used for plasmid annotation analysis. Subsequently, prodigal (v2.6.3), tRNAscan-SE-2.0 (http://trna.ucsc.edu/software/) and

Barrnap software (https://github.com/tseemann/barrnap) were used for the prediction of coding genes, tRNA, and rRNA, respectively. Interproscan (v5.25-64.0) was used to compare the predicted coding proteins with 6 databases, namely the Clusters of Orthologous Groups (COG), Kyoto Encyclopedia of Genes and Genomes (KEGG), Gene Ontology (GO), NR, Pfam, and Swiss-prot for functional annotation. Bowtie2 (v2.3.5) software (http://bowtie-bio.sourceforge.net/bowtie2/index.shtml) was used to annotate the high-quality sequences obtained after RNA sequencing. The AR612 genome sequence was used as the reference.

2.7 Whole genome alignment with transcriptome gene expression analysis

The whole-genome alignment of *L. salivarius* AR612 was performed using progressiveMAUVE (http://darlinglab.org/mauve/user-guide/introduction.html). A phylogenetic tree was constructed using MEGA software with the neighbour-joining method. RSEM (v1.3.1) (http://deweylab.github.io/RSEM/) was used to quantify transcript abundance, and the transcripts per million reads (TPM) method was used to estimate expression levels. DESeq2 (v1.24.0) software (http://bioconductor.org/packages/release/bioc/html/DESeq2.html) was used to perform differential expression analysis after transcript quantification. $P < 0.05$ and the absolute value of $\log_2$ (fold change (FC)) > 1 were used as the thresholds for significantly differentially expressed genes (DEGs).

2.8 Raw data deposit

The genome and plasmid sequences of *L. salivarius* AR612 were submitted to the NCBI database (https://submit.ncbi.nlm.nih.gov/about/genome/) with the following accession numbers: chromosome (CP123986) and plasmids (CP123987 and CP123988). The transcriptomic data of 18 samples were deposited in the Short Read Archive database (https://submit.ncbi.nlm.nih.gov/subs/sra) under the accession numbers SRR26908821 to SRR26908838.

2.9 Data analysis

Data integration and image processing were performed using Microsoft Excel 2016 and Adobe Photoshop CS5, respectively. All experiments were done in triplicate and all data were expressed as mean ± standard deviation. The analysis of variance (One-way ANOVA) and Duncan's multiple range test were used to verify the difference between the means of the variables analyzed in the experiments. Graphical representations were generated with Origin 2022 (OriginLab, Northampton, USA).

3. Results

3.1 Genome analysis

3.1 Genome features

The genome sequencing of *L. salivarius* AR612 provided detailed insights into its genetic composition (Table 1). The complete genome size was 1 970 245 bp with a GC content of 33.01%, comprising 1 chromosome and 2 plasmids. Table 2 lists the non-coding RNA and mobile elements identified in the genome. The AR612 genome contained 1 894 coding genes, 77 tRNA, 22 rRNA, and 36 sRNA. In addition, the genome contained various elements, such as 6 genomic islands (GI), 2 prophages (Ph), 2 CRISPR/Cas, 2 insertion sequences (IS), and 11 transposon sequences (Tns).

Table 1
Basic information of *L. salivarius* AR612.

Genome size (bp)	Chromosome	Plasmid	Total CDS number	Total length (bp)	Average length (bp)	Length/genome length (%)	GC content (%)
1 970 245	1	2	1 894	1 724 700	910.61	87.54	33.01

Table 2
Non-coding RNA and mobile genetic element statistics of *L. salivarius* AR612.

Type	Number	Average length (bp)	Total length (bp)	Percentage of genome (%)
Non-coding RNA				
tRNA	77	75.65	5 825	0.30
5S rRNA	8	110.25	882	0.04
16S rRNA	7	1 557.14	10 900	0.55
23S rRNA	7	2 912	20 384	1.03
sRNA	36	142.47	5 129	0.26
Mobile genetic element				
GI	6	21 297.67	127 786	6.49
Ph	2	16 625	33 250	1.69
CRISPR-Cas	2	783	1 566	0.08
IS	2	2 297.5	4 595	0.23
Tns	11	832.09	9 153	0.46

The gene function of *L. salivarius* AR612 was analysed using the KEGG, COG, and GO databases (Fig. 1). The integral component of membrane (328), cytoplasmic (233), and ATP-binding (217) were the 3 categories with the highest numbers of gene annotations in the GO database. Similarly, carbohydrate metabolism (130), membrane transport (92), and translation (81) were the 3 categories with the highest numbers of gene annotations in the KEGG database. Furthermore, translation, ribosomal structure and biogenesis (196), carbohydrate transport and metabolism (141), and amino acid transport and metabolism (138) were the 3 categories with the highest numbers of gene annotations in the COG database. The genome circle map created using CGview (https://proksee.ca/) provides a macroscopic view of the whole-genome characteristics of AR612, including its genome size, GC content, coding genes and non-coding RNAs. In addition, we compared AR612 with 4 other *L. salivarius* strains to determine their synteny differences (Fig. 2) and constructed

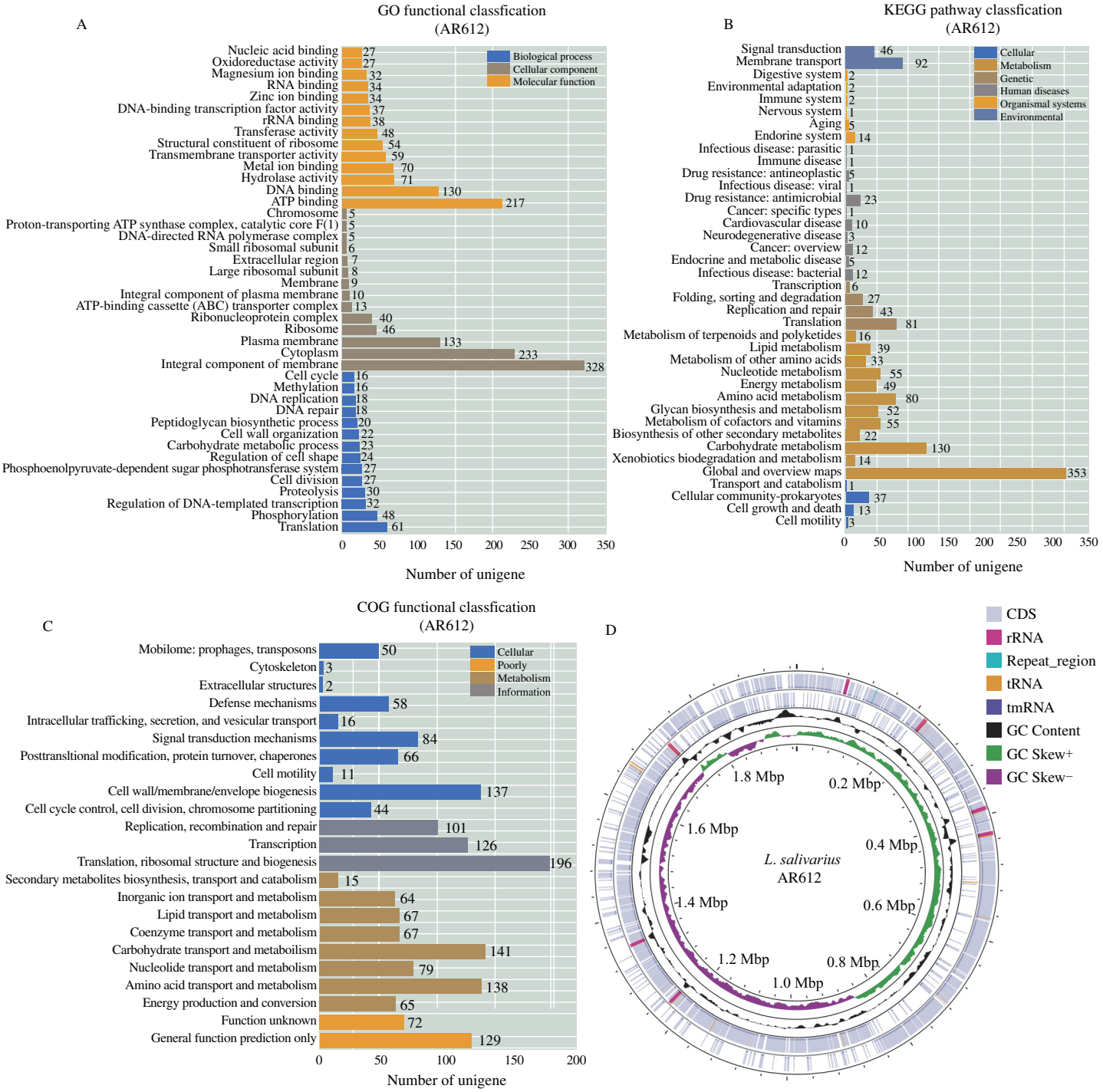

Fig. 1 Functional annotation of the *L. salivarius* AR612. (A) GO database annotation. (B) KEGG database annotation. (C) COG database annotation. (D) Genome circular map. From inside to outside are genome size, GC-Skew, GC content, tmRNA and all coding genes, forward stand gene, and reverse stand gene, respectively. (E) Phylogenetic tree of strain AR612 and references strains. The tree was constructed using software MEGA 7.0 by the neighbor-joining method, based on 16S rRNA gene sequences.

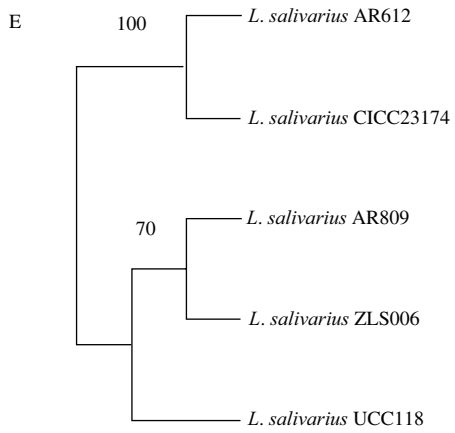

Fig. 1 (*Continued*)

a phylogenetic tree (Fig. 1E). The results of synteny analysis revealed that most of the regions in the AR612 genome were conserved within the species[15]. Compared with another *L. salivarius* strain, AR809, from our laboratory, AR612 exhibited rearrangements and multiple differential fragments in its genome (Fig. 2). Furthermore, phylogenetic analysis indicated that CICC23174 had the highest similarity to AR612 (Fig. 1E).

3.1.2 Stress-related protein analysis

L. salivarius AR612 contains abundant genes encoding stress-related proteins. The sources of stress include temperature, pH, osmotic pressure, bile, and oxidative stress (Table 3). These genes equip AR612 with robust capabilities to respond to external environmental changes and colonisation. Our previous study demonstrated that AR612 can tolerate a certain degree of acidic pH (4 to 5), lysozyme exposure, and hydrogen peroxide (data not shown). The acid resistance of AR612 may be related to the presence of a complete F0F1-ATPase proton pump system in its genome. A study indicated that the F0F1-ATPase proton pump, which is responsible for pH regulation, plays a key role in the acid and alkali resistance of LAB[16]. In addition, in AR612, 5 genes encoding sodium-proton antiporters and 2 genes encoding alkaline shock proteins further improved its acid resistance. Moreover, the genome contained 2 genes encoding cholylglycine hydrolase.

In addition to acid resistance, 2 osmotic stress-related genes and 23 oxidative stress-related genes were identified in the AR612 genome. These genes support the colonisation of AR612 in the oral-gastrointestinal tract. Furthermore, the genome contained 9 genes related to temperature stress, including *cspA*, *dnaJ*, *dnaK*, *grpE*, *htpX*, and *groES*. These findings provided a valuable reference for subsequent research into the stress resistance of AR612.

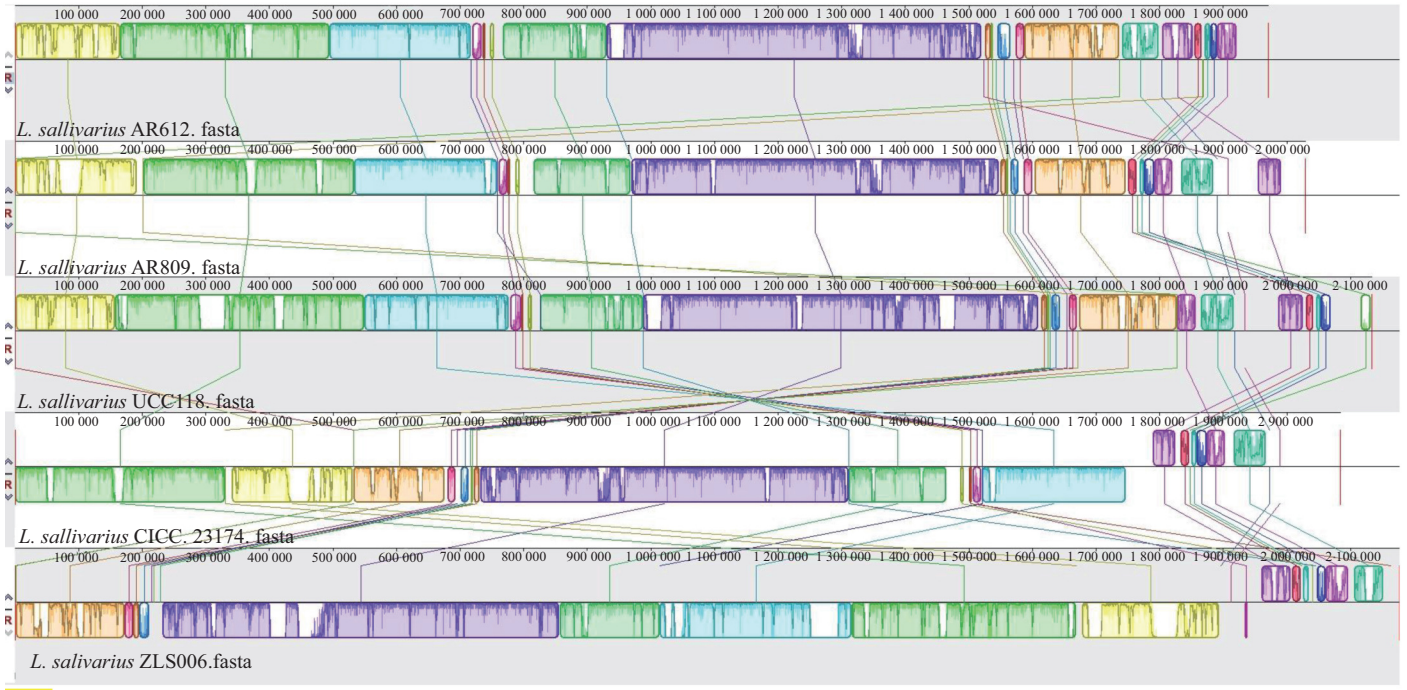

Fig. 2 MAUVE alignment of genomes from different *L. salivarius* strains and AR612 were set as a reference genome.

Table 3
Stress-related proteins of *L. salivarius* AR612.

Stresses	Stress-related proteins	Locus tag
Temperature	Cold shock protein CspA	Chr_orf1063, Chr_orf1468
	Heat shock protein DnaJ	Chr_orf0570
	Heat shock protein DnaK	Chr_orf0569
	Heat shock protein GrpE	Chr_orf0568
	Heat shock protein HtpX	Chr_orf0242
	Heat shock protein Hsp33	Chr_orf1363
	Ribosome-associated heat shock protein	Chr_orf1369
	Co-chaperonin GroES (heat shock protein)	Chr_orf1193
pH	Sodium-proton antiporters	Chr_orf0856, Chr_orf1388, Chr_orf1528, Chr_orf1631, Chr_orf0933, p612A_orf0130
	F0F1 ATP synthase	Chr_orf0584, Chr_orf0585, Chr_orf0586, Chr_orf0587, Chr_orf0588, Chr_orf0589, Chr_orf0590, Chr_orf0591
	Alkaline shock proteins	Chr_orf0522, Chr_orf0611
	CFP synthase	Chr_orf0947
Osmotic stress	Glycine/betaine ABC transporter, ATP-binding protein	p612B_orf0027, p612B_orf0028
Stress	ABC transporter, substrate binding and permease	Chr_orf0070, Chr_orf0573, Chr_orf1538
	ABC transporter, permease protein	Chr_orf0125, Chr_orf0126, Chr_orf0143, Chr_orf0152, Chr_orf0249, Chr_orf0472, Chr_orf0720, Chr_orf0882, Chr_orf0997, Chr_orf1446, Chr_orf1680, Chr_orf1681, p612A_orf0056, p612A_orf0110, p612B_orf0042
	Transport protein	Chr_orf1475, Chr_orf1648
	Manganese-dependent inorganic pyrophosphatase	Chr_orf0830
Bile	Cholylglycine hydrolase	Chr_orf0511, p612A_orf0052
Oxidative stress	Thiol peroxidase	Chr_orf1669
	Glutathione reductase	p612B_orf0026
	Glutaredoxin	Chr_orf1212
	NADH peroxidase	Chr_orf0148
	NADH oxidase	Chr_orf1628
	Thioredoxin	Chr_orf0889, Chr_orf1100, Chr_orf1463, Chr_orf1463, p612A_orf0118
	Thioredoxin reductase (NADPH)	Chr_orf1714
	Pyruvate oxidase	Chr_orf0018, Chr_orf1382
	Heavy metal translocating P-type ATPase	Chr_orf0176, Chr_orf1191, Chr_orf1601, Chr_orf1642, Chr_orf1687, p612A_orf0037
	Manganese transport protein	Chr_orf0905
	Manganese ABC transporter permease protein	Chr_orf1588
	Manganese ABC transporter ATP-binding protein	Chr_orf1589
	Manganese ABC superfamily ATP binding cassette transporter, substrate binding protein	Chr_orf1590

3.2 Effects of glucose stress on growth and acid production of L. salivarius AR612

As shown in Fig. 3, the stress environment caused by low or high glucose concentrations exerts varying effects on the activity and acid production of *L. salivarius* AR612. Under low glucose stress, because of the absence of a carbon source, the maximum growth of AR612 was significantly lower than that of the control group (20 g/L) (Fig. 3A). However, the lag phase was significantly shortened, and the maximum specific growth rate of AR612 was significantly higher than that of the control group. Conversely, under high glucose stress, the lag phase was significantly prolonged, and the maximum growth and specific growth rate of AR612 were lower than those of the control group. Fig. 3B presents the acid production ability of AR612 under low and high glucose stress in the logarithmic and stationary phases of the control group. In the logarithmic phase, AR612 grew rapidly under low glucose

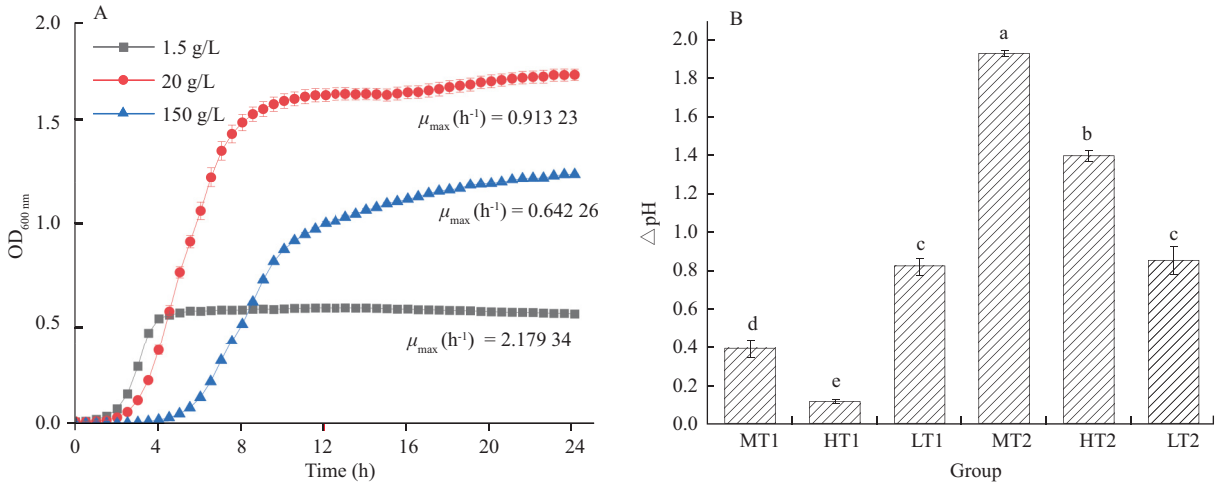

Fig. 3 Effects of glucose stress on growth and acid production of *L. salivarius* AR612. (A) Growth curve of *L. salivarius* AR612 under glucose stress. The red scale on the X-axis represents the sampling time point. (B) Acid production of *L. salivarius* AR612 under glucose stress. Different lowercase letters represent significant differences between groups ($P < 0.05$).

stress, and its acid production ability was significantly higher than that of the control group and the high glucose stress group. However, in the stationary phase, the limited carbon source in the low glucose group resulted in no change in the pH of the fermentation broth. In the high glucose group, the bacteria adapted to the stress environment, proliferating and reducing the pH rapidly; however, the decrease was still significantly lower than that in the control group.

3.3 Morphological differences analysis of L. salivarius AR612 under glucose stress

The cell surface morphology of *L. salivarius* AR612 under glucose stress is shown in Figs. 4 and S1. The control group exhibited smooth and regular cell morphology, whereas cells under glucose stress displayed irregular shapes or variations in size and length (Fig. 4). Specifically, under glucose stress, the division and length of AR612 cells increased when compared with the control group. In addition, under glucose stress, the cells appeared shrivelled and wrinkled (Figs. 4D and S1), with some becoming almost spherical. Under low glucose stress, the cell surface developed pores (Fig. S1).

As illustrated in Table 4, in the logarithmic phase, cell length and the length/diameter ratio significantly increased under high glucose stress compared with low glucose stress, and the maximum length was 2.43 μm. In the stationary phase, no significant differences in cell length and the length/diameter ratio were noted between the high glucose concentration and control groups. However, the cell length and length/diameter ratio of bacteria significantly increased in the low glucose concentration group compared with the high glucose concentration group, and the maximum length was 2.34 μm. The cell volume showed the same trend. The findings presented in both Fig. 4 and Table 4 indicate that changes in cell length or spherical morphology may be critical for bacterial survival and adaptation to nutritional stress.

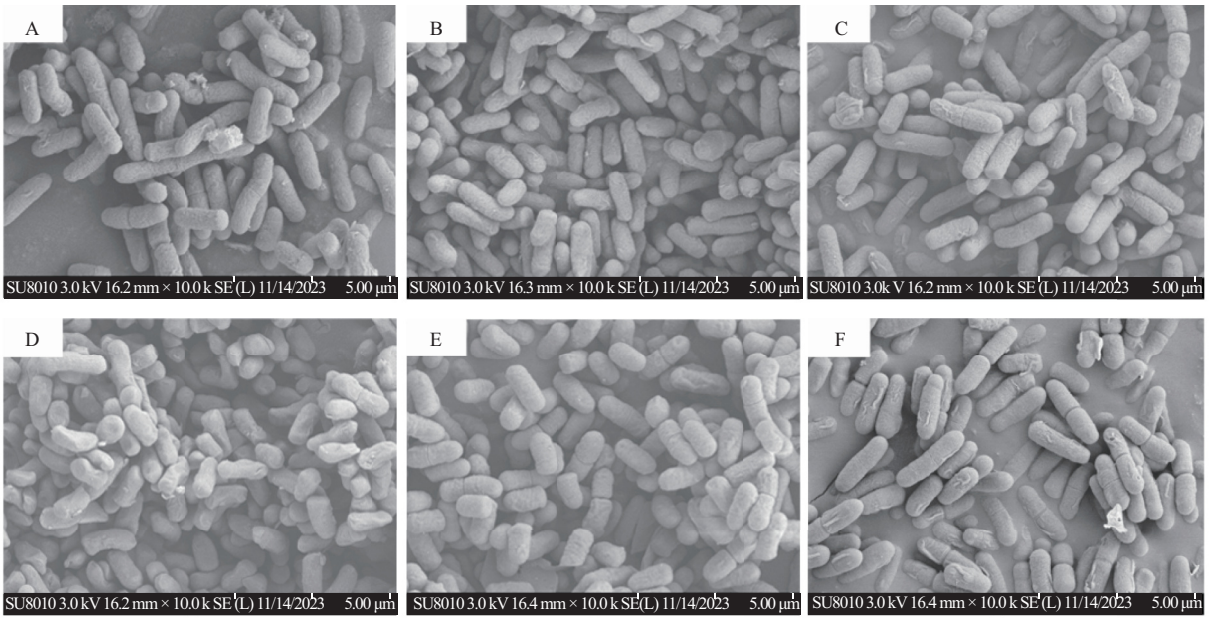

Fig. 4 Cell surface morphology of *L. salivarius* AR612 under different concentrations of glucose stress. (A) 150 g/L glucose, T1 stage; (B) 20 g/L glucose, control group at T1 stage; (C) 1.50 g/L glucose, T1 stage; (D) 150 g/L glucose, T2 stage; (E) 20 g/L glucose, control group at T2 stage; (F) 1.5 g/L glucose, T2 stage.

Table 4
Effect of nutrient stress on average cell length, diameter, length/diameter ratio and volume of *L. salivarius* AR612.

Group	Length (μm)	Diameter (μm)	Length/diameter	Volume ($μm^3$)
HT1	2.43 ± 0.72^{a}	0.63 ± 0.05^{bc}	3.84 ± 1.10^{a}	0.70 ± 0.27^{a}
MT1	1.59 ± 0.31^{c}	0.61 ± 0.07^{c}	2.67 ± 0.71^{bc}	0.40 ± 0.09^{c}
LT1	1.91 ± 0.39^{b}	0.63 ± 0.06^{bc}	3.07 ± 0.67^{b}	0.53 ± 0.16^{b}
HT2	1.53 ± 0.42^{c}	0.65 ± 0.07^{b}	2.40 ± 0.84^{c}	0.43 ± 0.12^{bc}
MT2	1.54 ± 0.26^{c}	0.71 ± 0.04^{a}	2.19 ± 0.40^{c}	0.51 ± 0.12^{b}
LT2	2.34 ± 0.31^{a}	0.62 ± 0.06^{bc}	3.79 ± 0.62^{a}	0.65 ± 0.15^{a}

Note: Different lowercase letters indicate significant differences ($P < 0.05$).

3.4 Effects of glucose stress on the transcriptome of L. salivarius AR612

3.4.1 Overview of transcriptome sequencing

To investigate the overall responses of *L. salivarius* AR612 to glucose stress, we conducted the transcriptome analysis of AR612 cells treated with different concentrations (150, 20, and 1.5 g/L) of glucose based on RNA sequencing. This analysis resulted in the generation of 30.87, 30.20, 29.34, 31.58, 30.58, and 29.92 million clean reads per library (Table S1). The percentage of reads with a quality score of ≥ Q30 exceeded 96% for all treatments, indicating that the sequencing data met the requirements for transcriptome analysis[17]. Furthermore, the alignment of the clean reads with the *L. salivarius* AR612 genome sequence revealed that more than 95% of the clean reads in each treatment mapped to unique positions in the reference genome.

3.4.2 DEGs analysis of L. salivarius AR612 transcriptome under glucose stress

To identify genes with altered transcript levels under glucose stress, we quantified the global transcript levels of the genes using the TPM method. The numbers of genes annotated in the GO, COG, KEGG, Pfam, NR, and Swiss-Prot databases were 1 423, 1 698, 1 236, 1 662, 2 061, and 1 534 for the entire transcriptome, respectively (Fig. 5A). We detected 1 810 and 1 283 genes in the T1 and T2 phases, respectively (Figs. 5B and C).

On the basis of the observed gene expression level of each sample, we identified DEGs between samples using DESeq2 for differential analysis. The results revealed that 97 DEGs were up-regulated and 17 DEGs were down-regulated in the LT1 group compared with the control group. Furthermore, 46 DEGs were up-regulated and 48 DEGs were down-regulated in the HT1 group compared with the control group. In addition, 495 DEGs were up-regulated and 472 DEGs were down-regulated in the LT2 group compared with the control group. Moreover, 189 DEGs were up-regulated and 258 DEGs were down-regulated in the HT2 group compared with the control group (Fig. 5D). To better illustrate the effects of glucose stress on AR612, we constructed a Venn diagram of the distribution of DEGs in the 3 groups (Fig. S2). We identified 10 and 97 DEGs for the 3 glucose concentrations at the T1 and T2 periods, respectively. These findings indicated that *L. salivarius* AR612 undergoes complex transcriptional regulation under glucose stress in the stable period. Numerous genes that are relatively silent in the logarithmic phase appear to be abnormally active in the stationary phase.

3.5 Modular analysis of glucose stress response by L. salivarius AR612

To analyse the transcriptional response mechanism of AR612 to glucose stress, we performed a modular analysis of the DEGs of AR612 under different glucose treatment conditions, including genes related to cell growth morphology, carbohydrate metabolism, amino acid metabolism, fatty acid synthesis, nucleotide synthesis, and stress-related proteins.

3.5.1 Effects of glucose stress on genes related to cell morphology

In this study, we identified several genes associated with the cell morphology of *L. salivarius* AR612 and observed variations in their expression; the results are presented in Table 5. The *acm* gene that encodes a cellular hydrolase has previously been demonstrated to play an important role in cell division in *Lactiplantibacillus plantarum*[18-19]. As shown in Table 5, the expression of *acm* was down-regulated by 0.64- and 4.90-fold in the HT1 and HT2 groups compared with the control group. However, the expression of *acm* was up-regulated by 0.03- and 0.85-fold in the LT1 and LT2 groups compared with the control group. The *ezrA* and *ftsA* genes encode proteins related to cell division. EzrA is a membrane-associated protein involved in the coordination of cell division and cell wall synthesis in Gram-positive bacteria[20]. The expression of *ezrA* was down-regulated by 0.38- and 1.15-fold in the T1 and T2 periods compared with the control group, respectively. Furthermore, the expression of *ftsA* was down-regulated by 0.19- and 1.38-fold in the T1 and T2 periods compared with the control group. The *jag* and *orf0622* genes encode 2 cytoplasmic RNA-binding proteins that form a heterogeneous complex in the middle of a cell[21-22]. At the transcriptional level, glucose stress inhibits the formation of the heterogeneous complex in the early logarithmic phase. These results indicated that glucose stress affects the expression of genes related to AR612 cell morphology, thereby influencing the morphology of the bacterium.

3.5.2 Effects of glucose stress on carbohydrate metabolism

Four main systems are responsible for carbohydrate transport in LAB cells: the phosphotransferase transporter system (PTS), ABC transporter, permease, and symporter[23]. Fig. S3 shows differences in the expression of the 4 transporter systems under glucose stress. During the T1 period, AR612 mainly used the PTS, ABC transporter and permease for exogenous glucose uptake. Most of the PTS genes

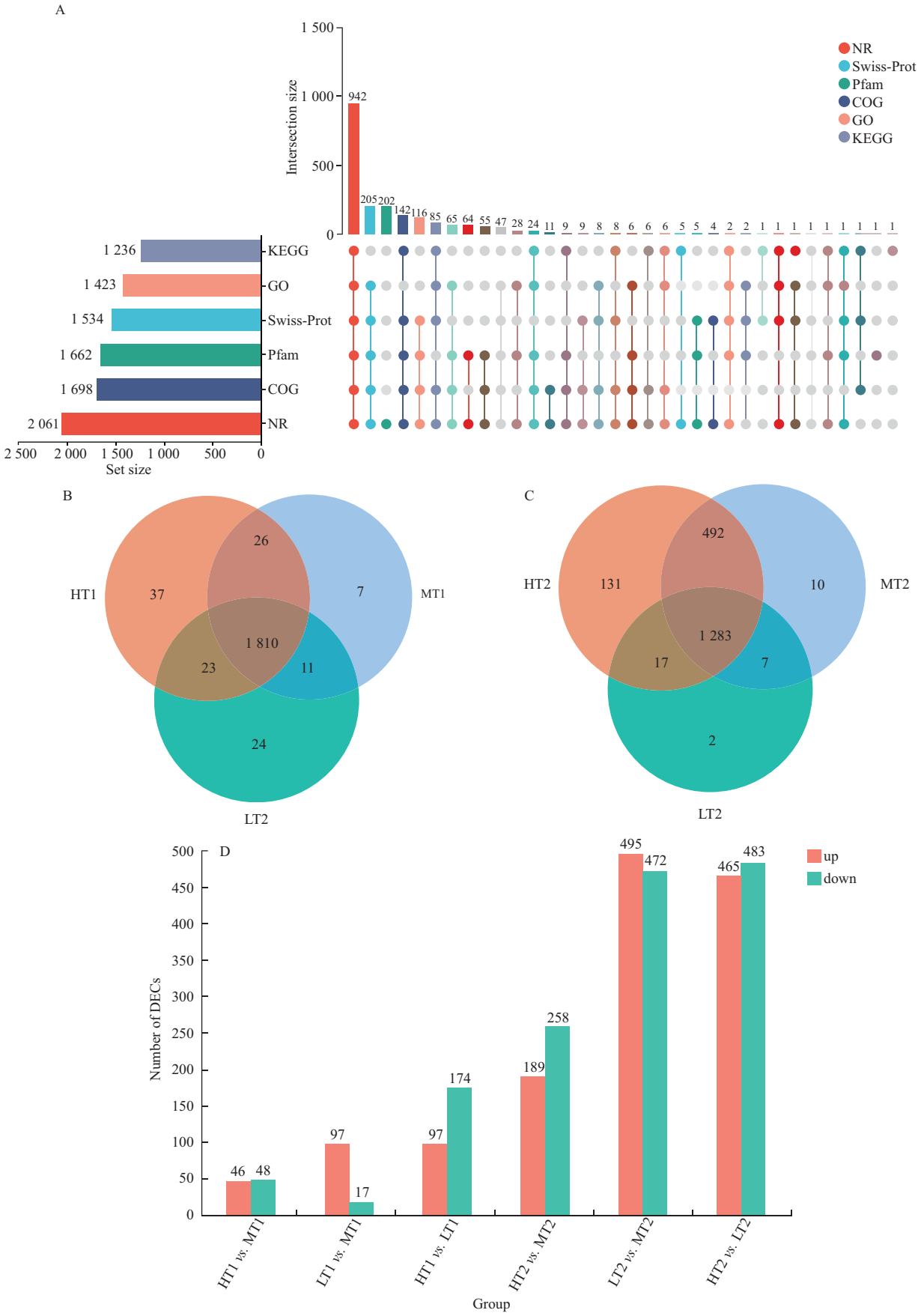

Fig. 5 DEGs analysis of *L. salivarius* AR612 transcriptome under glucose stress. (A) Venn diagram of the unigenes annotated to the NR, Swiss-Prot, Pfam, KEGG, COG, and GO. (B-C) Distribution Venn diagram of unigenes in different groups. (D) Distribution histogram of DEGs.

Table 5
Effect of nutrient stress on average cell length, diameter, length/diameter ratio and volume of *L. salivarius* AR612.

Gene_ID	Gene name	Description	HT1 *vs.* MT1[a]	LT1 *vs.* MT1	HT1 *vs.* LT1	HT2 *vs.* MT2	LT2 *vs.* MT2	HT2 *vs.* LT2
orf0793	*acm*	Glycoside hydrolase, a cell wall hydrolase	−0.64	0.03	−0.67	−4.90	0.85	−5.74
orf0001	*dnaA*	DNA replication, initiator protein	0.43	0.05	0.39	0.94	−1.22	2.18
orf1069	*ezrA*	Early cell division protein	0.17	−0.38	0.56	0.27	−1.15	1.43
orf1042	*ftsA*	Cell division protein	0.24	−0.19	0.44	0.44	−1.38	1.84
orf0594	*mreB*	Rod shape-determining protein	0.12	0.32	−0.19	0.22	−0.46	0.70
orf1062	*mreB*	Rod shape-determining protein	0.18	0.00	0.19	0.59	−1.37	1.98
orf1650	*jag*	RNA-binding cell elongation regulator	0	0.3	−0.29	0.2	−0.24	0.46
orf0622	–	KH domain-containing protein	−0.22	−0.62	0.42	0.49	1.25	−0.73
orf1488	–	Coordinator of zonal elongation	0.03	−0.07	0.11	1.10	−0.37	1.49
orf0333	–	Coordinator of zonal elongation	0.04	−0.3	0.36	−1	−1.51	0.54

Note: Represents the ratio of $\log_2$ FC. − indicates that the gene has no corresponding gene name in the KEGG annotation.

were down-regulated in the HT1 group compared with the HT2 group, with *manX*, *mtlA*, and *cmtB* being significantly down-regulated by 1.16-, 1.47-, and 1.2-fold in the HT1 group, respectively. In contrast to HT1, most carbohydrate transporter genes were up-regulated under low glucose stress, including the gene cluster *manXYZ* encoding the mannose/fructose/sorbose cluster. During the T2 period, the expression of PTS genes, such as *bglF*, *manXYZ*, *ptsI*, *scrA*, and *cmtB* significantly increased under high glucose stress. In addition, AR612 mainly used the PTS and ABC transporter for glucose uptake in the T2 stage. Furthermore, glucose deprivation led to a significant decrease in the expression of permease system genes. These findings indicated that glucose stress affects the ability of AR612 to take up glucose during the exponential and stabilisation phases, prompting AR612 to regulate the expression of genes related to carbohydrate transport for maintaining glucose homeostasis.

To further determine the differential expression of genes related to carbohydrate metabolism under glucose stress, we mapped the relevant genes to different carbohydrate metabolism pathways (Fig. 6). Under high glucose stress, most of the metabolic genes involved in various pathways, such as the glycolysis pathway, fructose and mannose metabolism, and pyruvate metabolism, were down-regulated in the T1 period compared with the control group, including *fbaA*, *ccpA*, *zwf*, and *pfkA*. However, genes related to fructose and mannose metabolism and TCA cycle pathways were all up-regulated in the T2 stage, including *fruK*, *scrK*, *manA*, and *pckA*. By contrast, in the LT1 group, most genes were up-regulated, including *galM*, *bglA*, *ackA*, and *pflD*. In the stationary phase, most genes were significantly down-regulated, including *pgi*, *glk*, and *pyk*. In addition, compared with low glucose stress, high glucose stress reduced gene expression in the logarithmic phase, and most genes were upregulated in the stationary phase. These findings indicated that under low glucose stress, AR612 activates genes related to carbohydrate metabolism to overcome challenges associated with glucose deprivation. Conversely, under high glucose stress, AR612 inhibits the expression of genes involved in carbon source metabolism and reduces glucose uptake and utilisation.

3.5.3 Effect of glucose stress on amino acid metabolism

During the fermentation process of LAB, amino acids serve as essential nutrients that support the normal growth of strains and enhance their environmental tolerance. We analysed the differential expression of genes involved in amino acid metabolism pathways in AR612 under glucose stress (Fig. 7, Table S2).

Glutamate and glutamine act as nitrogen sources for bacterial cells and play a crucial role in nitrogen metabolism. In this study, all relevant genes involved in glutamate metabolism in AR612 were down-regulated in the log phase under high glucose stress, including glutamate-cysteine ligase (orf0065, *gshA*), glutamyl-tRNA synthetase (orf0997), and glutamine synthetase (orf1629). However, all these genes were upregulated during the stabilisation period. Many amino acids in Gram-positive bacteria are involved in the modification and assembly of cell wall and cell membrane components. The protein encoded by *dltA* is responsible for catalysing the acylation of alanine to lipophosphatidic acid. Under glucose stress, *dltA* (orf0893) transcript levels were up-regulated in all groups, except the HT1 group, when compared with the control group. Thus, we hypothesised that the stress capacity of AR612 is enhanced through an increase in the acylation of LTA. In addition, under glucose stress, several enzymes involved in the aspartate-to-lysine pathway were up-regulated in the log phase, including aspartate-semialdehyde dehydrogenase (orf0270, *asd*), pyridoxal phosphate-dependent aminotransferase (orf0835, *patA*), and 4-hydroxy-tetrahydrodipicolinate synthase/reductase (orf0633/orf0700, *dapA*/*B*). However, the expression of related genes in the low glucose group was down-regulated in the stable phase. Furthermore, the transcriptional levels of the related enzymes involved in the synthesis of threonine, another amino acid in the aspartic acid family, were altered under glucose stress. This finding suggested that AR612 responds to glucose stress by altering the expression of genes involved in amino acid metabolism.

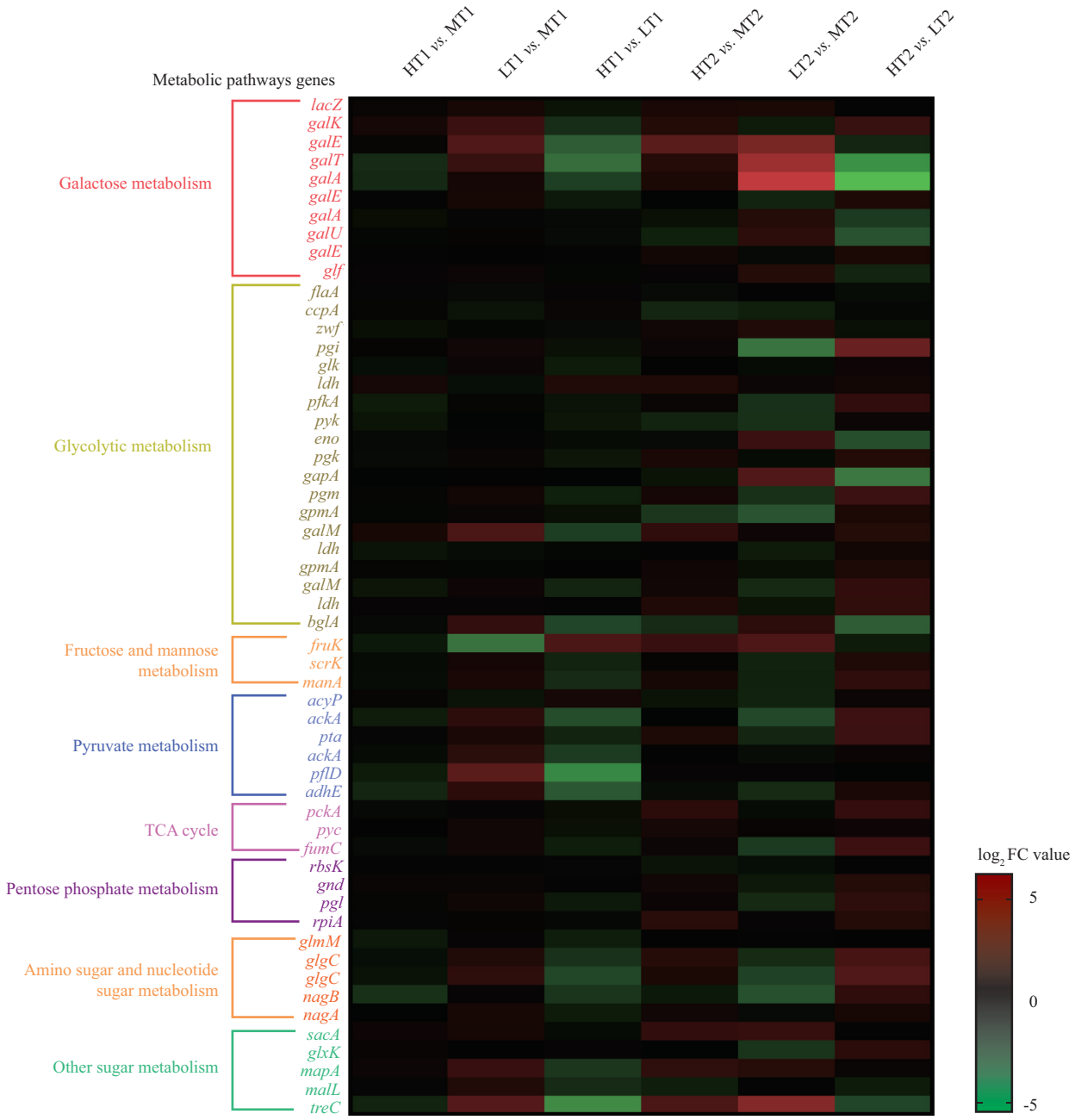

Fig. 6 Effect of glucose stress on carbohydrate metabolism was analyzed by heat map.

3.5.4 *Effect of glucose stress on fatty acid synthesis*

The transcript levels of genes involved in fatty acid synthesis in AR612 changed under glucose stress, and the results are shown in Fig. 8. Genes involved in the fatty acid synthesis pathway (*accABCD* and *fabDFGHIZ*) were significantly down-regulated in the high glucose stress group compared with the control group, indicating that the overall synthesis of fatty acids in the cells was slowed under high glucose stress. A similar finding was noted in the low glucose stress group. However, in the low glucose stress group, genes involved in fatty acid synthesis were up-regulated during the stationary phase. These findings indicated that glucose stress can alter fatty acid synthesis in AR612, thereby affecting bacterial growth.

3.5.5 *Effect of glucose stress on nucleotide metabolism*

Purine nucleotides are crucial metabolites in cells. They are essential components of DNA and RNA and act as energy carriers for various intracellular metabolism through ATP and GTP. In addition, purine nucleotides are involved in the synthesis and metabolism of intracellular amino acids and vitamins. The results of this study revealed that the expression of some genes (e.g. *purCDHMN*) involved in purine metabolism was up-regulated in the high glucose stress group compared with the control group, whereas *purA* was down-regulated in both T1 and T2 periods under high glucose stress (Fig. 9). In contrast to the high glucose stress group, most of the genes involved in purine metabolism were down-regulated under low glucose stress.

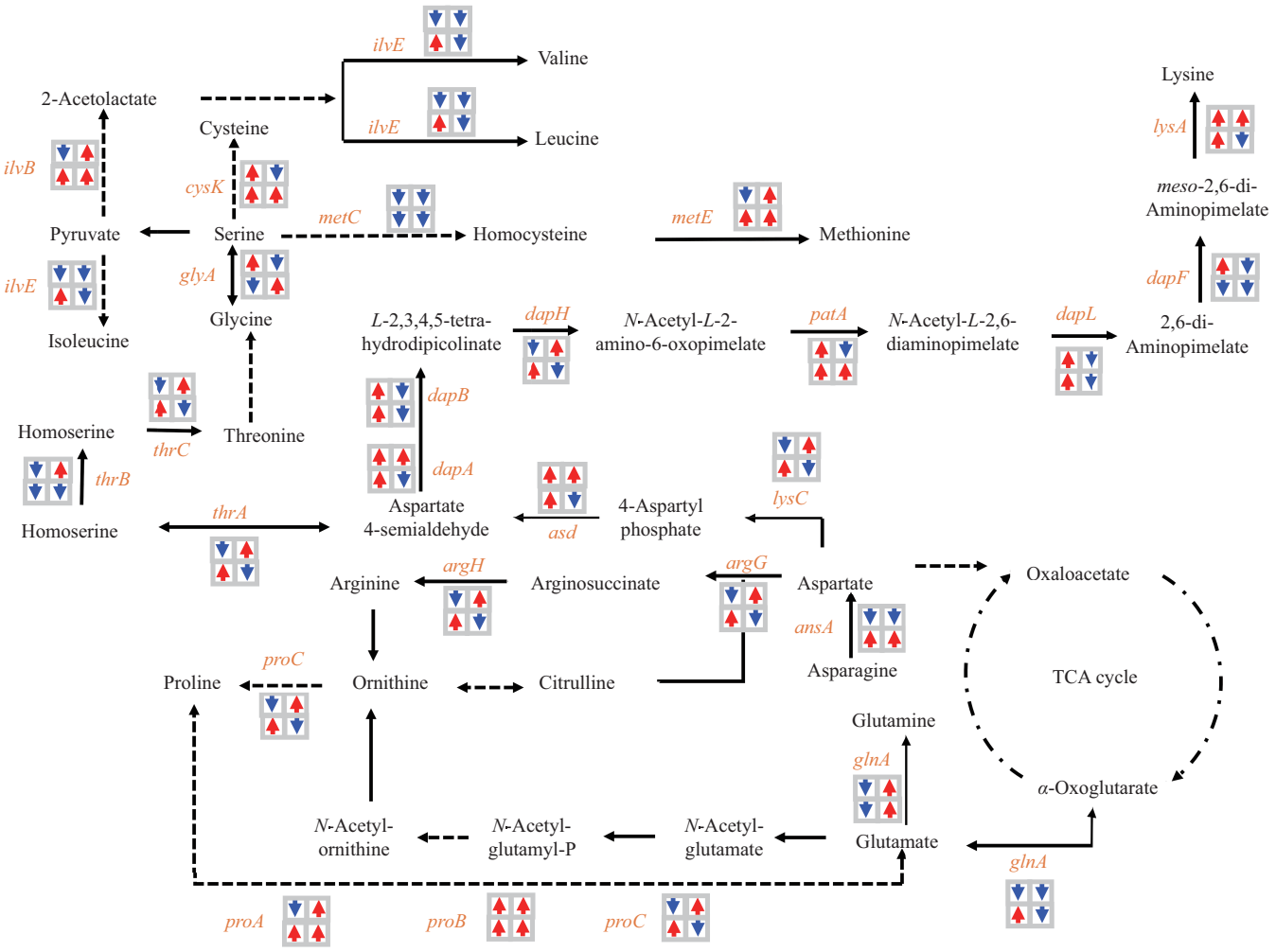

Fig. 7 DEGs involved in amino acid biosynthesis under glucose stress. The top and bottom rows of boxes on the left side represent the relative expression of genes in the high glucose concentration group. The right side represents the low glucose concentration group.

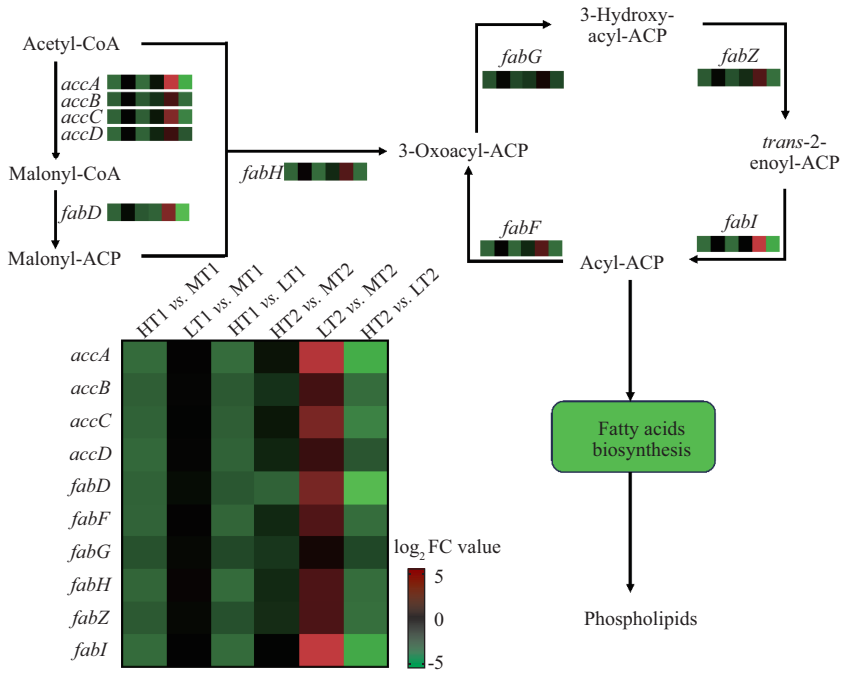

Fig. 8 Effect of glucose stress on fatty acid synthesis pathway in *L. salivarius* AR612.

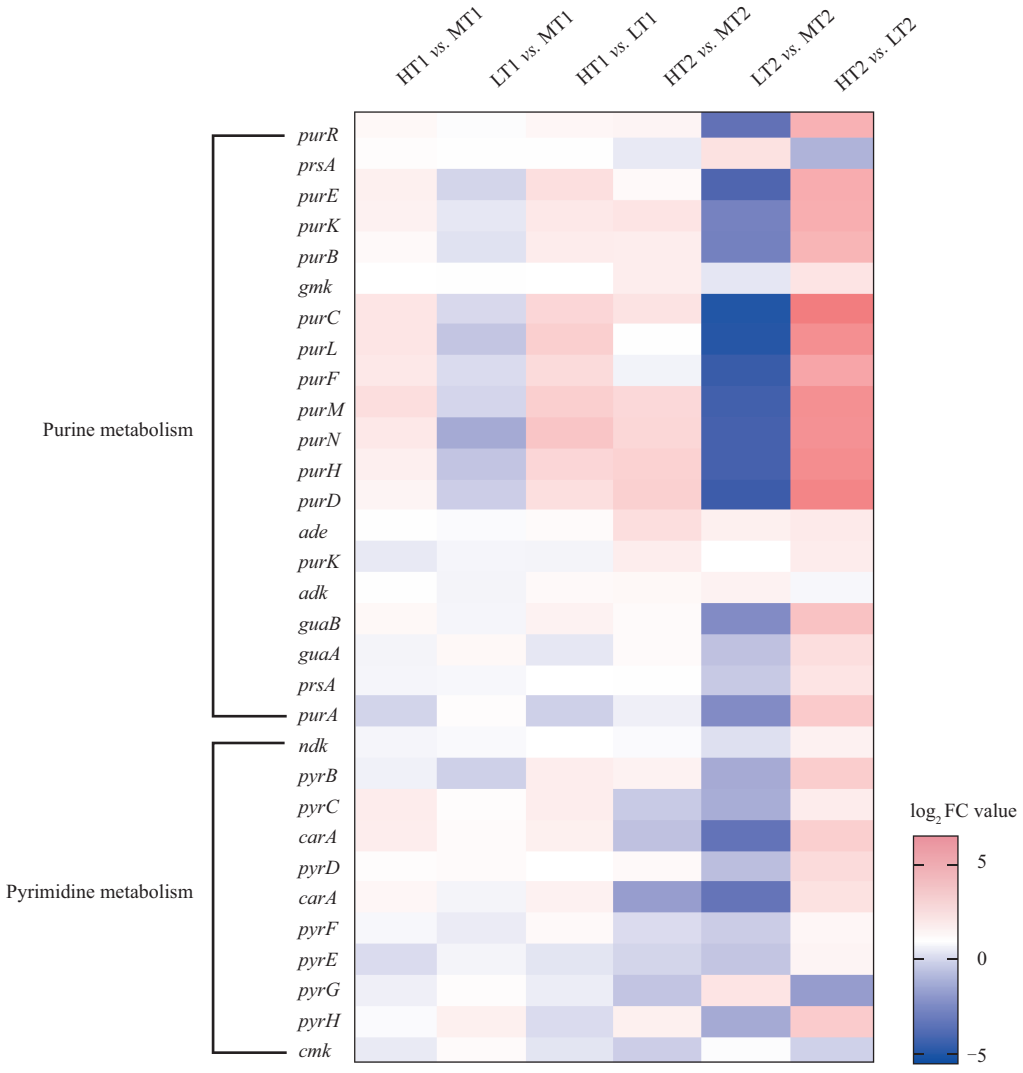

Fig. 9 Effect of glucose stress on nucleotide metabolism was analyzed by heat map.

The *de novo* pyrimidine synthesis pathway begins with the formation of carbamoyl phosphate from glutamate, catalysed by carbamoyl phosphate synthetase,which is encoded by *carA*. Subsequently, the *pyrBCDEF* gene cluster catalyses the conversion to UMP. Aspartic transcarbamoylase is encoded by *pyrC*, an important rate-limiting gene in this process. Under high glucose stress, *carA* and *pyrC* were up-regulated during the T1 period but down-regulated during the T2 period (Fig. 9). Under low glucose stress, the expression of *carA* and *pyrC* did not change during the T1 period but was down-regulated during the T2 period. These results indicated that during the T1 period, high glucose stress may enhance cellular nucleic acid replication and confer resistance to hyperosmotic stress.

3.5.6 Effects of glucose stress on genes encoding stress proteins

We examined the effect of glucose stress on genes encoding stress-related proteins (Table 3). Among them, most genes related to temperature stress proteins were down-regulated under glucose stress, including *cspA*, *dnaJ*, and *dnaK*. F0F1 ATP synthase plays a crucial role in the regulation of acid balance by probiotics. Under high glucose stress, AR612 was in a growth-inhibited state during the T1 phase, exhibiting a weak acid-production ability, and the F0F1 ATP synthase gene was down-regulated. During the T2 phase, as AR612 adapted to the hypertonic environment and bacterial proliferation increased, the pH declined rapidly and the F0F1 ATP synthase gene was up-regulated. The effect of low glucose stress on AR612 was weaker than that of high glucose stress. Similar to *L. plantarum*, *L. salivarius* AR612 also has a glycine-betaine system. Genes involved in this system were up-regulated during the T1 period under glucose stress and down-regulated during the T2 period. Furthermore, oxidative stress induced by glucose stress caused differential changes in gene expression in AR612. The findings indicate that glucose stress affects the expression of stress-related genes in AR612.

3.5.7 iPath global analysis of differential genes

The metabolic, regulatory, and secondary metabolite biosynthesis pathways involved in DEGs were visualised and analysed using iPath. This approach helped to illustrate the metabolic pathway information of the entire biological system under glucose stress (Fig. 10). The metabolic pathways involving DEGs under glucose stress were

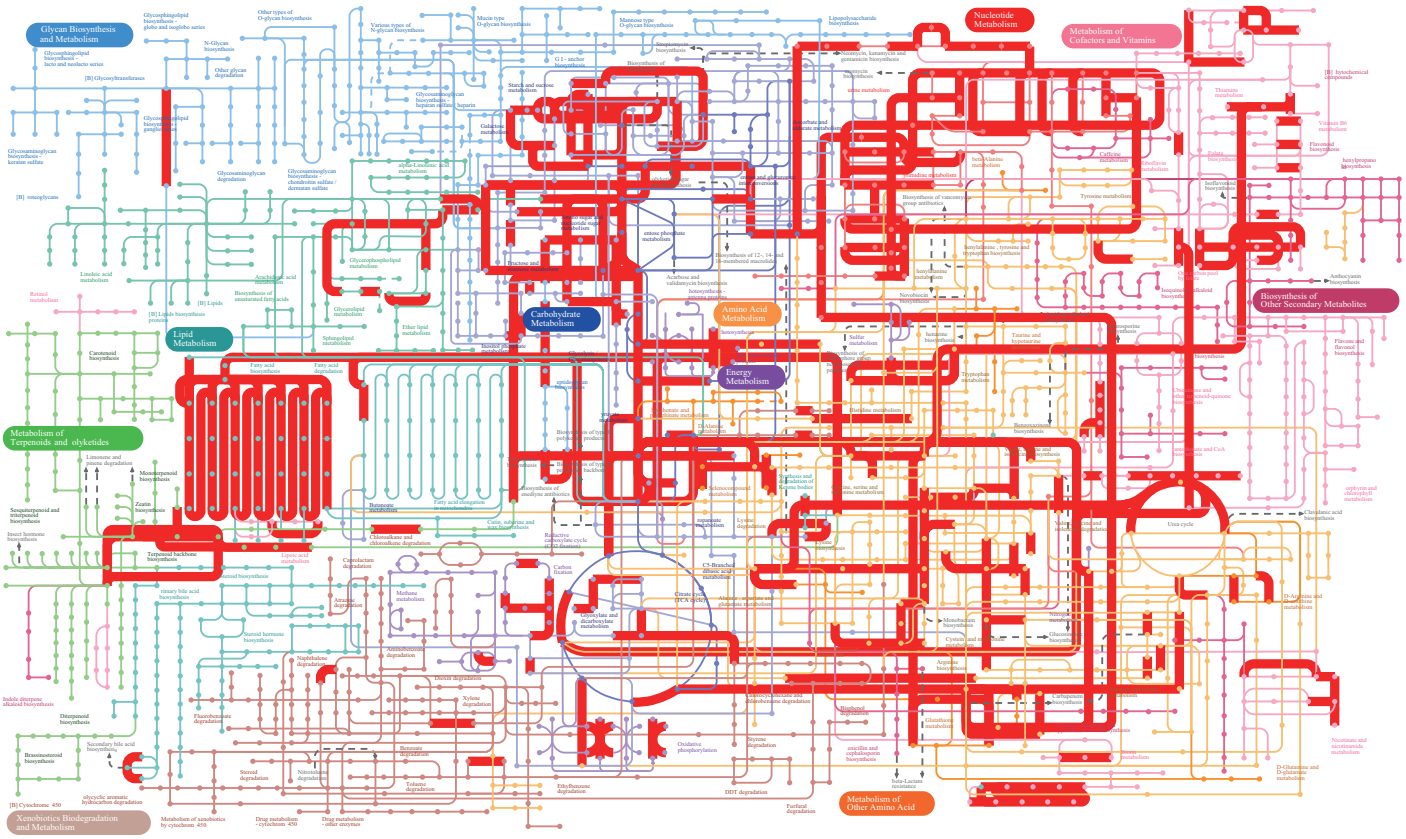

Fig. 10 Analysis of significant DEGs using iPath (https://pathways.embl.de/ipath3.cgi) metabolic pathways between the control group and glucose stress group. Red line indicate differential gene annotation pathways.

mainly fatty acid synthesis, carbohydrate metabolism, amino acid metabolism, and nucleotide metabolism. The regulatory pathways involved were mainly DNA replication and repair, ribosomal and aminoacyl-tRNA biosynthesis in translation, and PTS and ABC transport in membrane transport (Fig. S4).

4. Discussion

Probiotics play an important role in human health, such as by aiding in the digestion and absorption of nutrients such as lactose and protein[24-25], regulating immune functions, reducing inflammatory factor levels, increasing the immunoglobulin content[26], lowering cholesterol levels[27], maintaining host intestinal homeostasis, and preventing intestinal diseases[28]. However, nutritional stress is a crucial environmental challenge that probiotics must overcome for survival. The adaptation mechanisms, genetic profiles, and functional gene alterations of probiotics in response to physiological and environmental changes can be comprehensively analysed using multi-omics methods, including genomics, transcriptomics, metabolomics, proteomics, and synthetic biology. AR612 is a probiotic *L. salivarius* strain that we previously isolated from infant faeces. In this study, we analysed the response mechanism of AR612 to glucose stress through whole-genome and transcriptome sequencing. Previously, our laboratory performed the whole-genome sequencing of another *L. salivarius* strain, AR809, and identified numerous genes encoding stress-related proteins, such as those associated with pH, temperature, osmotic pressure, bile salts, and oxidative stress[16]. Our results revealed that the genome of *L. salivarius* AR612 contained 1 970 245 bp with a GC content of 33.01% and 1 894 coding genes. In addition, through genome annotation, we identified a series of genes encoding stress-related proteins in the AR612 genome through annotation, which provides some clues for the subsequent study of the mechanism of AR612's response to glucose stress.

Currently, our knowledge regarding how LAB adapts to nutritional stress is still considerably fragmented and usually focuses on glycolysis and LAB survival[29]. Glucose is the main source of carbon and energy for LAB, and glucose stress typically occurs during the fixed stage of LAB growth. Redon et al.[30] indicated that adaptation to carbon starvation in LAB is mediated by 3 types of responses: an overall response, a specific response related to glucose depletion, and other reactions that have never been described previously in the context of carbon starvation. Functions related to bacterial growth are generally decreased in the overall response. In this study, we first investigated the effects of glucose stress on the growth of AR612 cells by analysing the growth curve, acid production ability, and cell morphology. The results are consistent with the overall response. Under glucose stress, the lag phase was significantly prolonged and the maximum growth was significantly decreased. Morphological changes are crucial indicators of LAB stress and survival mechanisms. Parlindungan et al. examined morphological changes in *L. plantarum* B21 cells under glucose and Tween 80 stress[13]. In line with the findings reported by Parlindungan et al.[13], we observed that nutritional stress can lead to cells becoming irregular in shape and size. When the bacterial morphology changes from a rod or spiral form to a spherical form, the integrity of the bacterial cell membrane is generally believed to prevent its internal structure

from the influence of the external environment, and its genetic material remains intact while maintaining a low metabolic activity rate[31-32]. Therefore, AR612 responds to glucose stress in its environment through morphological changes.

Typically, pronounced phenotypic or functional differences between samples are often attributed to large variations in gene expression. On the basis of phenotypic changes induced by glucose stress, we used transcriptomics to examine alterations in gene expression in AR612. Under high glucose stress, the growth of AR612 was severely inhibited. In the early stage, we noted weak carbohydrate metabolic activity, including the glycolysis pathway, fructose and mannose metabolism, and pyruvate metabolism. In the stationary phase, AR612 adapted to the hyperosmotic environment, leading to the accumulation of cells in large quantities and the up-regulation of carbohydrate transporter genes, thereby activating some metabolic pathways (e.g. sugar and mannose metabolism and the TCA cycle pathway) and influencing global regulation. In addition, the expression levels of *pfkA* (encoding phosphofructokinase) and *pyk* (encoding pyruvate kinase) were low and did not change significantly. As key rate-limiting enzymes in the glycolysis pathway[33], their low activity may contribute to the slow glycolysis rate observed under high glucose stress. In the low glucose stress group, most genes were up-regulated during the logarithmic phase. In the stationary phase, when the cells were starved, we noted a significant down-regulation in transcription. This finding indicated that AR612 activates genes related to carbohydrate metabolism under low glucose stress to manage glucose deficiency. Conversely, under high glucose stress, AR612 inhibits the expression of genes involved in carbon source metabolism and reduces glucose uptake and utilisation, resulting in the inhibition of the growth of AR612.

Amino acids are involved in many physiological functions of cells. Under stress conditions, amino acids can accumulate in large quantities and act as protective agents[9]. In this study, under high glucose stress, the expression of genes involved in amino acid metabolism in the stationary phase was generally increased. Conversely, under low glucose stress, most of the genes involved in amino acid metabolism were down-regulated. Studies have indicated that a substantial carbon source deficiency can prompt LAB to enter the stationary phase prematurely. However, because glucose is consumed in the later growth stage, to ensure survival, cells begin to use other sugars or amino acids during this phase[7,34]. This may explain the general down-regulation of genes involved in amino acid metabolism under low glucose stress. In addition, genes involved in cysteine-methionine metabolism were up-regulated in the early stage under glucose stress. Cysteine and methionine can help in scavenging ROS and reducing oxidative stress[35]. Thus, enhancing the transport of methionine and cysteine may play a role in resisting oxidative stress induced by high glucose levels. Lysine modifications are critical for cell membrane integrity[36]. In the stationary phase, the up-regulation of *lysA* expression in the high glucose group, which may increase the lysylation modification of membrane phospholipids, may contribute to morphological differences between the high and low glucose groups (Fig. S1). Proline, a protective amino acid, is critical in microbial responses to external stressful environments[37]. The *proABC* gene, which is responsible for proline synthesis, was up-regulated during the stabilisation phase in the high glucose group in this study. This finding indicated that proline is a key amino acid involved in the response of AR612 to osmotic stresses.

A study reported that the cell size and fatty acid composition of LAB can vary under the growth conditions adapted to glucose stress[38]. The composition and distribution of fatty acids directly affect the fluidity of the cell membrane[39], influencing the transmembrane transport of nutrients and the acquisition of energy in a stressful environment. Zhang et al.[40] proposed that LAB can change the composition and content of fatty acids in their cell membranes as a strategy to adapt to the stress environment. Cell membrane fluidity is regulated by changes in the ratio of unsaturated fatty acids to saturated fatty acids, thus reducing damage under nutritional stress. Furthermore, hyperosmotic stress can alter cell membrane structure and cytoplasmic enzyme activities, adversely affecting the normal physiological function of the strain[41]. In this study, we observed the differential expression of genes involved in fatty acid synthesis in AR612, influencing cell membrane structure and related components; this finding was verified by the morphological changes in AR612. In addition, some genes encoding stress-related proteins changed significantly in response to glucose stress.

Nucleotides are essential for all organisms, and they serve as substrates for RNA and DNA synthesis. They can also generate energy through the interconversion of ATP, ADP, AMP, GTP, GDP, and GMP and are the most important energy supplier of cells. Whole-genome analysis revealed the presence of enzymes related to the purine synthesis pathway in *L. salivarius* AR612. Beyer et al.[42] reported that in the early stage of fermentation, genes involved in the *de novo* synthesis pathway of purine were highly expressed. However, our results showed different trends. In our study, genes involved in the purine synthesis pathway were up-regulated in the high glucose stress group but inhibited in the low glucose stress group in the early stage of fermentation. This may be due to the presence of adequate exogenous purine compounds in the medium, and the strain preferentially uses exogenous purine compounds, resulting in a decrease in the reactivity of related metabolic pathways. Derzelle et al.[43] indicated that exogenous purine can be internalised by strains and inhibit the expression of genes related to the *de novo* synthesis of purine. In this study, in the stationary phase, the purine synthesis pathway was inhibited in the low glucose stress group, which may be related to the decreased growth activity of the strain at this time. For all organisms, the pyrimidine nucleotides CTP and UTP and their derivatives are essential growth elements. Transcriptomics results revealed that the expression of genes involved in the pyrimidine synthesis pathway was similar to the expression of genes involved in purine metabolism, indicating that glucose stress affects nucleotide metabolism in AR612.

Given the widespread use of *L. salivarius* in various fields, understanding its metabolic kinetics under glucose stress is crucial. Investigating gene expression changes in *L. salivarius* under different glucose stress levels can provide valuable data for enhancing our understanding of the genetic characteristics of *L. salivarius*.

5. Conclusion

L. salivarius has various excellent probiotic properties. In this study, genomic and transcriptomic analyses revealed that certain genes (including encoding stress proteins) may be related to its probiotic properties and genetic adaptation. Moreover, we examined differences

in morphology and gene expression in AR612 under glucose stress through transcriptome sequencing. Integrative analysis showed that *L. salivarius* AR612 may respond to glucose stress through altering the expression of genes involved in various cellular and metabolic processes, including cell division, RNA binding, carbohydrate metabolism, amino acid metabolism nucleotide metabolism, and fatty acid synthesis. The iPath regulatory pathway analysis identified differential gene annotation pathways, indicating the involvement of specific regulatory pathways in the response to glucose stress. These results can aid in the construction of the gene regulatory network of *L. salivarius* under glucose stress, providing valuable insights for further study of the molecular mechanism underlying the response of *L. salivarius* to glucose stress. Our findings can also inform the development of stress-resistant probiotic LAB strains and the optimization of industrial production. Finally, this study promotes the use of sequencing technology to study the resistance of other microorganisms and host organisms to environmental stress. In summary, using genomics and transcriptomics to analyse the response mechanisms of *L. salivarius* to nutritional stress can not only enrich our understanding of its biological characteristics but also promote the development of related technologies and the application of *L. salivarius* in various industries, indicating its scientific value and practical significance.

Declaration of interests

All authors declared that they have no conflicting interest.

Acknowledgements

This work was supported by the Natural Science Foundation of China (32272364), the Shanghai Education Committee Scientific Research Innovation Projects, China (2101070007800120), National Science Foundation for Distinguished Young Scholars (32025029), Shanghai Key Project in Synthetic Biology (23HC1400900), and the Shanghai Engineering Research Center of 460 Food Microbiology Program (19DZ2281100).

Appendix A. Supplementary data

Supplementary data associated with this article can be found, in the online version, at http://doi.org/10.26599/FSHW.2024.9250350.

References

[1] Y.R. Lee, W.Y. Bang, K.R. Baek, et al., Safety evaluation by phenotypic and genomic characterization of four *Lactobacilli* strains with probiotic properties, Microorganisms 10 (2022) 2218. https://doi.org/10.3390/microorganisms10112218.

[2] P. Vidhate, P. Wakchoure, S. Borole, et al., *Lactobacillus* as probiotics: opportunities and challenges for potential benefits in female reproductive health, Am. J. Transl. Res. 16 (2024) 720-729. https://doi.org/10.62347/IGWR5474.

[3] T. Feng, J. Wang, Oxidative stress tolerance and antioxidant capacity of lactic acid bacteria as probiotic: a systematic review, Gut Microbes 12 (2020) 1801944. https://doi.org/10.1080/19490976.2020.1801944.

[4] X.W. Gao, J. Kong, H.K. Zhu, et al., *Lactobacillus*, *Bifidobacterium* and *Lactococcus* response to environmental stress: mechanisms and application of cross-protection to improve resistance against freeze-drying, J. Appl. microbiol. 132 (2022) 802-821. https://doi.org/10.1111/jam.15251.

[5] H. Wang, B.D. Ha, I.H. Kim, Effects of probiotics complex supplementation in low nutrient density diet on growth performance, nutrient digestibility, faecal microbial, and faecal noxious gas emission in growing pigs, Ital. J. Anim. Sci. 20 (2021) 163-170. https://doi.org/10.1080/1828051X.2020.1801358.

[6] C. Dressaire, E. Redon, C. Gitton, et al., Investigation of the adaptation of *Lactococcus lactis* to isoleucine starvation integrating dynamic transcriptome and proteome information, Microb. Cell Fact. 10 (2011) S18. https://doi.org/10.1186/1475-2859-10-S1-S18.

[7] I. Yoon, M. Nam, H.K. Kim, et al., Glucose-dependent control of leucine metabolism by leucyl-tRNA synthetase 1, Science 367 (2020) 205-210. https://doi.org/10.1126/science.aau2753.

[8] H.X. Wang, J.Q. Tang, J.Y. Lv, et al., Physiological and transcriptomic insights into sugar stress resistance in osmophilic yeast *Zygosaccharomyces rouxii*, Food Microbiol. 117 (2024) 104395. https://doi.org/10.1016/j.fm.2023.104395.

[9] L. Pan, J. Yu, D.Y. Ren, et al., Metabolomic analysis of significant changes in *Lactobacillus casei* Zhang during culturing to generation 4,000 under conditions of glucose restriction, J. Dairy Sci. 102 (2019) 3851-3867. https://doi.org/10.3168/jds.2018-15702.

[10] J. Yu, W.Y. Hui, C.X. Cao, et al., Integrative genomic and proteomic analysis of the response of *Lactobacillus casei* Zhang to glucose restriction, J. Proteome Res. 17 (2018) 1290-1299. https://doi.org/10.1021/acs.jproteome.7b00886.

[11] E.Panel o.B. Hazards, K. Koutsoumanis, A. Allende, et al., Update of the list of QPS-recommended biological agents intentionally added to food or feed as notified to EFSA 13: suitability of taxonomic units notified to EFSA until September 2020, EFSA J. 19 (2021) e06377. https://doi.org/10.2903/j.efsa.2021.6377.

[12] Y. Yang, X. Song, G.Q. Wang, et al., Understanding *Ligilactobacillus salivarius* from probiotic properties to omics technology: a review, Foods 13 (2024) 895. https://doi.org/10.3390/foods13060895.

[13] E. Parlindungan, C. Dekiwadia, B.K. May, et al., Nutrient stress as a means to enhance the storage stability of spray dried microencapsulated *Lactobacillus plantarum* B21, LWT-Food Sci. Technol. 111 (2019) 204-210. https://doi.org/10.1016/j.lwt.2019.05.010.

[14] E. Parlindungan, C. Dekiwadia, K.T.M. Tran, et al., Morphological and ultrastructural changes in *Lactobacillus plantarum* B21 as an indicator of nutrient stress, LWT-Food Sci. Technol. 92 (2018) 556-563. https://doi.org/10.1016/j.lwt.2018.02.072.

[15] T. Huang, T. Xiong, Z. Peng, et al., Genomic analysis revealed adaptive mechanism to plant-related fermentation of *Lactobacillus plantarum* NCU116 and *Lactobacillus* spp, Genomics 112 (2020) 703-711. https://doi.org/10.1016/j.ygeno.2019.05.004.

[16] Y. Yang, X. Song, Z.Q. Xiong, et al., Complete genome sequence of *Lactobacillus salivarius* AR809, a probiotic strain with oropharyngeal tract resistance and adhesion to the oral epithelial cells, Curr. Microbiol. 79 (2022) 280. https://doi.org/10.1007/s00284-022-02963-w.

[17] R. Pei, G. Lv, B. Guo, et al., Physiological and transcriptomic analyses revealed the change of main flavor substance of *Zygosaccharomyces rouxii* under salt treatment, Front. Nutr. 9 (2022) 990380. https://doi.org/10.3389/fnut.2022.990380.

[18] M.C. Duchêne, T. Rolain, A. Knoops, et al., Distinct and specific role of NlpC/P60 endopeptidases LytA and LytB in cell elongation and division of *Lactobacillus plantarum*, Front. Microbiol. 10 (2019) 713. https://doi.org/10.3389/fmicb.2019.00713.

[19] I.S. Myrbraten, K. Wiull, Z. Salehian, et al., CRISPR interference for rapid knockdown of essential cell cycle genes in *Lactobacillus plantarum*, mSphere 4 (2019) e00007-19. https://doi.org/10.1128/mSphere.00007-19.

[20] C.S. Wassmann, P. Højrup, J.K. Klitgaard, Cannabidiol is an effective helper compound in combination with bacitracin to kill Gram-positive bacteria, Sci. Rep. 10 (2020) 4112. https://doi.org/10.1038/s41598-020-60952-0.

[21] A.R. Winther, M. Kjos, G.A. Stamsås, et al., Prevention of EloR/KhpA heterodimerization by introduction of site-specific amino acid substitutions renders the essential elongasome protein PBP2b redundant in *Streptococcus pneumoniae*, Sci. Rep. 9 (2019) 3681. https://doi.org/10.1038/s41598-018-38386-6.

[22] A.R. Winther, M. Kjos, M.L. Herigstad, et al., EloR interacts with the lytic transglycosylase MltG at midcell in *Streptococcus pneumoniae* R6, J. Bacteriol. 203 (2021). https://doi.org/10.1128/jb.00691-20.

[23] G. Liu, Y. Qiao, Y. Zhang, et al., Metabolic profiles of carbohydrates in *Streptococcus thermophilus* during pH-controlled batch fermentation, Front. Microbiol. 11 (2020) 1131. https://doi.org/10.3389/fmicb.2020.01131.

[24] J. Wang, H. Ji, Influence of probiotics on dietary protein digestion and utilization in the gastrointestinal tract, Curr. Protein Pept. Sc. 20 (2019) 125-131. https://doi.org/10.2174/1389203719666180517100339.

[25] J. Teichenné, Ú. Catalán, R. Mariné-Casadó, et al., *Bacillus coagulans* GBI-30, 6086 (BC30) improves lactose digestion in rats exposed to a high-lactose meal, Eur. J. Nutr. 62 (2023) 2649-2659. https://doi.org/10.1007/s00394-023-03183-z.

[26] J. Plaza-Díaz, F.J. Ruiz-Ojeda, L.M. Vilchez-Padial, et al., Evidence of the anti-inflammatory effects of probiotics and synbiotics in intestinal chronic diseases, Nutrients 9 (2017) 555. https://doi.org/10.3390/nu9060555.

[27] P. Zhao, M.X. Li, X. Mo, et al., Development and properties evaluation of multi-strain probiotic with cholesterol-lowering potential *in vitro*, Lett. Appl. Microbiol. 76 (2023) ovad038. https://doi.org/10.1093/lambio/ovad038.

[28] D.Y. Liu, C.Y. Li, T. Cao, et al., *Bifidobacterium longum* K5 prevents enterohaemorrhagic *Escherichia coli* O157:H7 infection in mice through the modulation of the gut microbiota, Nutrients 16 (2024) 1164. https://doi.org/10.3390/nu16081164.

[29] B. Ganesan, M.R. Stuart, B.C. Weimer, Carbohydrate starvation causes a metabolically active but nonculturable state in *Lactococcus lactis*, Appl. Environ. Microb. 73 (2007) 2498-2512. https://doi.org/10.1128/AEM.01832-06.

[30] E. Redon, P. Loubiere, M. Cocaign-Bousquet, Transcriptome analysis of the progressive adaptation of *Lactococcus lactis* to carbon starvation, J. Bacteriol. 187 (2005) 3589-3592. https://doi.org/10.1128/jb.187.10.3589-3592.2005.

[31] S.W. Chiu, S.Y. Chen, H.C. Wong, Localization and expression of MreB in *Vibrio parahaemolyticus* under different stresses, Appl. Environ. Microb. 74 (2008) 7016-7022. https://doi.org/10.1128/AEM.01020-08.

[32] S.J. Krebs, R.K. Taylor, Nutrient-dependent, rapid transition of *Vibrio cholerae* to coccoid morphology and expression of the toxin co-regulated pilus in this form, Microbiology 157 (2011) 2942-2953. https://doi.org/10.1099/mic.0.048561-0.

[33] X. Song, C.J. Hou, Y. Yang, et al., Effects of different carbon sources on metabolic profiles of carbohydrates in *Streptococcus thermophilus* during fermentation, J. Sci. Food Agr. 102 (2022) 4820-4829. https://doi.org/10.1002/jsfa.11845.

[34] J. Wang, W. Zhang, Z. Zhong, et al., Gene expression profile of probiotic *Lactobacillus casei* Zhang during the late stage of milk fermentation, Food Control 25 (2012) 321-327. https://doi.org/10.1016/j.foodcont.2011.10.036.

[35] J.H. Kim, H.J. Jang, W.Y. Cho, et al., *In vitro* antioxidant actions of sulfur-containing amino acids, Arab. J. Chem. 13 (2020) 1678-1684. https://doi.org/10.1016/j.arabjc.2017.12.036.

[36] G.H. Wang, Z.Y. Zhai, F.Z. Ren, et al., Combined transcriptomic and proteomic analysis of the response to bile stress in a centenarian-originated probiotic *Lactobacillus salivarius* Ren, Food Res. Int. 137 (2020) 109331. https://doi.org/10.1016/j.foodres.2020.109331.

[37] Y. Zhang, B.Y. Mao, X. Tang, et al., Integrative genome and metabolome analysis reveal the potential mechanism of osmotic stress tolerance in *Bifidobacterium bifidum*, LWT-Food Sci. Technol. 159 (2022) 113199. https://doi.org/10.1016/j.lwt.2022.113199.

[38] J. Ma, Z. Jiang, R. Jiang, et al., Physiological characteristics of nutrient stressed *Lactobacillus plantarum* KLDS 1.0328 and storage stability of its freeze-dried cells, Food Science 42 (2021) 155-161. (In Chinese) https://doi.org/10.7506/spkx1002-6630-20200712-156.

[39] Z.B. He, X.N. Zhang, R.Y. Sun, et al., Effects of three different gas environments on the storage stability of *Lactobacillus plantarum* LIP-1 at room temperature, Food Biosci. 44 (2021) 101391. https://doi.org/10.1016/j.fbio.2021.101391.

[40] Q.L. Zhang, L.L. Ma, J.J. E, et al., Effects of initial pH on heat resistance of *Lactobacillus plantarum* LIP-1, LWT-Food Sci. Technol. 138 (2021) 110748. https://doi.org/10.1016/j.lwt.2020.110748.

[41] X.Y. Wang, H. Wu, L.J. Wang, et al., Global transcriptional and translational regulation of *Sphingomonas melonis* TY in response to hyperosmotic stress, Environ. Res. 219 (2023) 115014. https://doi.org/10.1016/j.envres.2022.115014.

[42] N.H. Beyer, P. Roepstorff, K. Hammer, et al., Proteome analysis of the purine stimulon from *Lactococcus lactis*, Proteomics 3 (2003) 786-797. https://doi.org/10.1002/pmic.200300416.

[43] S. Derzelle, A. Bolotin, M.Y. Mistou, et al., Proteome analysis of *Streptococcus thermophilus* grown in milk reveals pyruvate formate-lyase as the major upregulated protein, Appl. Environ. Microbiol. 71 (2005) 8597-8605. https://doi.org/10.1128/AEM.71.12.8597-8605.2005.